

# Hopping conductivity and insulator-metal transition in films of touching semiconductor nanocrystals

Han Fu,<sup>1,\*</sup> K. V. Reich,<sup>1,2</sup> and B. I. Shklovskii<sup>1</sup>

<sup>1</sup>*Fine Theoretical Physics Institute, University of Minnesota, Minneapolis, MN 55455, USA*

<sup>2</sup>*Ioffe Institute, St Petersburg, 194021, Russia*

(Dated: May 28, 2022)

This paper is focused on the the variable-range hopping of electrons in semiconductor nanocrystal (NC) films below the critical doping concentration  $n_c$  at which the insulator-metal transition occurs. The hopping conductivity  $\sigma$  is described by the Efros-Shklovskii law as  $\sigma = \sigma_0 \exp[-(T_{ES}/T)^{1/2}]$  where  $T_{ES} \propto \xi^{-1}$  and  $\xi$  is the localization length of electrons. We study how the localization length  $\xi(n)$  grows with the doping concentration  $n$  in the film of touching NCs. This allows us to find the critical concentration  $n_c$ . Films with different kinds of contacts between neighboring NCs are discussed.

## I. INTRODUCTION

Semiconductor nanocrystals (NCs) have a great potential for optoelectronics applications such as solar cells<sup>1</sup>, light emitting diodes<sup>2</sup> and field effect transistors<sup>3,4</sup>. Their advantage is size-tunable optical and electrical properties<sup>5</sup> and low-cost solution-based processing techniques<sup>6,7</sup>. These applications require conducting NC films and several ways of introducing carriers via doping are being explored<sup>3,8-14</sup>. At a given concentration of carriers one tries to improve the mobility by moving NCs closer to each other and reducing their contact resistance.

In many studies<sup>8-11</sup> the low temperature conductivity of doped films was found to obey Efros-Shklovskii (ES) variable range hopping law<sup>15</sup>:

$$\sigma(T) = \sigma_0 \exp \left[ - \left( \frac{T_{ES}}{T} \right)^{1/2} \right]. \quad (1)$$

Here  $\sigma_0$  is a conductivity prefactor,  $T$  is the temperature, and

$$T_{ES} = \frac{Ce^2}{\varepsilon_f k_B \xi}, \quad (2)$$

in Gaussian units.  $e$  is the electron charge,  $\xi$  is the localization length,  $\varepsilon_f$  is the effective dielectric constant of the film,  $k_B$  is the Boltzmann constant,  $C \simeq 9.6$ <sup>16</sup>. Typically,  $\xi$  grows with the concentration of electrons  $n$  in a NC and the improvement of contacts between NCs. Therefore,  $T_{ES}$  becomes smaller and the film becomes more conducting<sup>10</sup>.

In this paper we concentrate on doping of NC films by chemical donors or acceptors<sup>17</sup> which was recently achieved in InAs<sup>13</sup>, CdSe<sup>14</sup> and Si<sup>10</sup> NCs. While many experimental studies have been directed towards increasing the conductivity of NC films with increased  $n$ , it was not clear when  $\xi$  diverges and  $T_{ES}$  vanishes so that the NC film becomes metallic<sup>18-20</sup>. In other words, what is the critical concentration  $n_c$  of electrons (or donors) in a NC necessary for the insulator-metal transition (IMT)? Recently<sup>10</sup>  $n_c$  was estimated for the favorable case of the

IMT, where close-to-spherical NCs touch each other by small facets of radius  $\rho \ll d$  without any ligands that impede the conduction creating a barrier between NCs (see Fig. 1a). The result is very simple

$$n_c \simeq 0.3\rho^{-3}. \quad (3)$$

The IMT is illustrated in Fig. 1a where we show how the electron wave packet of the minimum available size ( $\sim n^{-1/3}$ ) for a given  $n$  passes between two touching NCs at  $n > n_c$  ( $n^{-1/3} < \rho$ ), but gets stuck so that the electron has to tunnel at  $n < n_c$  ( $n^{-1/3} > \rho$ ).

Contacts between NCs may have different origins. For example, for close-to-spherical NCs, a facet is imposed by the discreteness of the crystal lattice and its radius can be approximated as  $\rho_a = \sqrt{da}/2$ , where  $a$  is the lattice constant and  $d$  is the NC diameter. For CdSe NCs with  $a = 0.6$  nm and  $d = 5$  nm, Eq. (3) gives  $n_c = 2 \times 10^{20} \text{ cm}^{-3}$ . For the case in which NCs shown in Fig. 1a touch each other away from these facets, a finite tunneling distance  $b \sim 0.1$  nm in the medium between NCs should be taken into account. This leads to an effective “ $b$ -contact” of radius  $\rho_b \ll \rho_a$  and a much larger critical concentration  $n_c$ . On the other hand, it was shown in Ref. 16 that at very light doping when the number of electrons per NC is less than unity one should see the nearest-neighbor hopping between NCs with the activation energy equal to the charging energy of an NC. This prediction is confirmed by the data of lightly doped Si NCs<sup>21</sup>. Thus, the ES hopping should be observed in a large range of the concentrations  $1/d^3 < n < n_c$ . To calculate  $T_{ES}$  given by Eq. (2), we need to know how the localization length  $\xi(n)$  grows in this range, before reaching the NC diameter  $d$  and diverging in a critical vicinity of  $n_c$ .

In this paper we show that if NCs touch by contact facets of radius  $\rho$ , the localization length  $\xi$  is

$$\xi(n) \approx \frac{d}{\ln(2/n\rho^3)}. \quad (4)$$

This result is obtained at low temperatures when electrons hop via the elastic multi-step co-tunneling

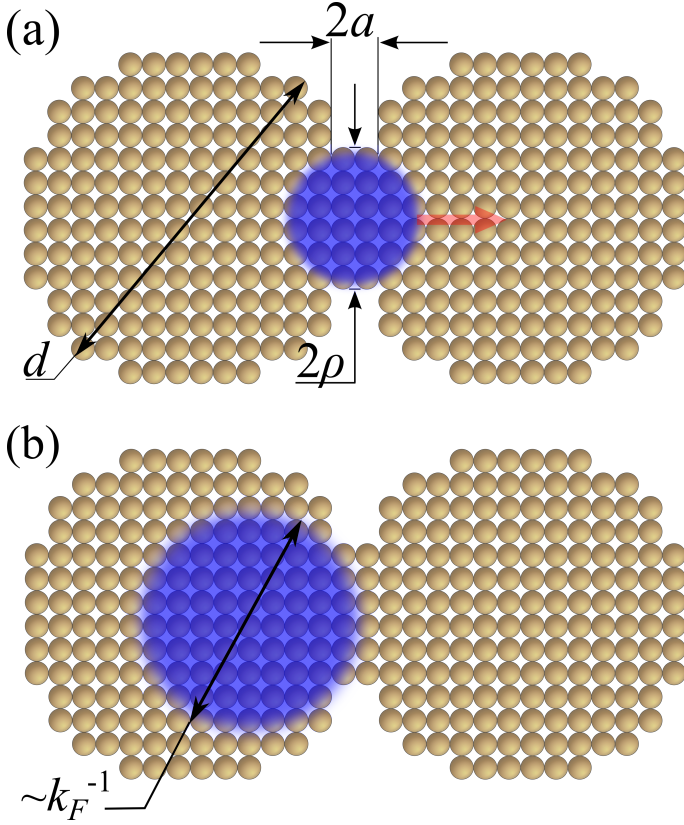


FIG. 1. (Color online) The cross-section of two NCs in contact by their facets with radius  $\rho \ll d$  each. Here  $a$  is the lattice constant,  $d$  is the NC diameter. The blue cloud depicts the smallest available electron wave packet with the size  $\sim k_F^{-1} \sim n^{-1/3}$ , where  $k_F$  is the Fermi wavenumber and  $n$  is the doping concentration of electrons in each NC. (a) Electron transport at  $n > n_c$ . The smallest electron packet fits in the touching facets and moves through the contact. (b) At  $n < n_c$ , the smallest wave packet gets stuck near the contact and the electron tunneling between NCs is depleted so much that it is not strong enough to overcome the disorder potential in order to delocalize electrons.

between distant NCs. We deal with the generic case when energy shells of the electron spectrum of the spherical NCs are weakly split by the disorder resulting from random donor positions in NCs. We show below that in this case, the effective dielectric constant  $\epsilon_f$  is not affected by the electron polarization in NCs far from the IMT. Therefore, together with Eq. (2), Eq. (4) can be used to predict the dependence  $T_{ES}(n)$ .

Using that  $\xi$  becomes comparable to  $d$  when  $n$  gets close to the critical concentration  $n_c$  of the IMT, we arrive from the insulating side at the estimate Eq. (3) which was obtained in Ref. 10 from the metallic side. This could be anticipated from the fact that in Eq. (4) the localization length  $\xi$  depends only on the product  $n\rho^3$ .

The paper is organized as follows. In Sec. II, we dwell upon the properties of a single NC inside an array of

touching NCs such as the quantization energy gap  $\Delta$  separating consecutive degenerate shells of the electron spectrum and the charging energy  $E_c$  of each NC. In Sec. III, we explain how NCs are charged due to variations of the donor number from NC to NC. In Sec. IV, we show that in most realistic cases, the splitting of degenerate electron energy shells by disorder due to random donor positions can be ignored. In Sec. V we give the expression of the localization length  $\xi$  in terms of the ratio of the tunneling matrix element  $t$  between neighboring NCs to the energy gap  $\Delta$ . In Sec. VI we calculate the tunneling matrix element  $t$  for NCs touching by contact facets (see Fig. 1b) and find  $\xi$  as a function of the doping concentration  $n$  (Eq. 4). In Sec. VII, we study the case where NCs touch each other away from prominent facets or are separated by short ligands and derive the corresponding expressions of  $\xi$ . We conclude in Sec. VIII.

## II. PROPERTIES OF A SINGLE NC IN AN ARRAY OF TOUCHING NANOCRYSTALS

We assume that these close-to-spherical NCs have diameter  $d$  and touch each other by facets with radius  $\rho$ . At small enough  $\rho$  electrons are localized inside NCs. We suppose that the electron wave function is close to zero at the NC surface, due to large confining potential barriers created by the insulator matrix surrounding the NC. Under these conditions, electrons occupy states with different radial and angular momentum quantum numbers, i.e.,  $(n, l)$ -shells each being degenerate with respect to the azimuthal quantum number  $m = -l, \dots, l$  where the polar axis ( $z$  axis) is defined in the direction of electron tunneling connecting centers of two neighboring NCs (we talk more about this in Sec. VI). As we explained in Introduction we are interested in NCs of which the average number of electrons is  $N \gg 1$ . Therefore several  $(n, l)$ -shells are occupied. The quantum energy gap between two consecutive  $(n, l)$ -shells typically is

$$\Delta \simeq \frac{20\hbar^2}{m^* d^2} \quad (5)$$

where  $m^*$  is the effective electron mass inside NCs.

Also, when the quantum numbers are large, Bohr's correspondence principle allows us to consider quasiclassically the average density of states of electrons and introduce the Fermi wave vector  $k_F$

$$k_F = (3\pi^2)^{1/3} n^{1/3}. \quad (6)$$

Here  $n = 6N/\pi d^3$  is the density of electrons in an NC. Below,  $k_F$  serves as an approximate measure of the concentration  $n$ .

The kinetic energy of electrons is only a part of the total energy of the NC. One should add to it the total Coulomb interaction energy of all electrons and donors. In general, calculating the total Coulomb

energy (self-energy) of the system is a difficult problem because of the random position of donors. For our case, however, a significant simplification is available because the semiconductor dielectric constant  $\varepsilon$  is typically much larger than the dielectric constant  $\varepsilon_m$  of the medium in which the NC is embedded. This allows us to ignore in a first approximation the energy dependence on positions of donors and electrons and instead concentrate on only the dependence of energy on the total charge of the NC  $Qe$ . We will discuss the role of disorder due to random donor positions in Sec. IV.

The energy of a NC with charge  $Qe$  surrounded by neutral NCs (i.e., the self-energy) is equal to  $Q^2 E_c$ , where the charging energy is

$$E_c = \frac{e^2}{\varepsilon_f d}. \quad (7)$$

For non-touching NCs where the volume fraction of semiconductor NCs is  $f \leq 0.52$ , one can use the Maxwell-Garnet formula<sup>22</sup>

$$\varepsilon_f = \varepsilon_m \frac{\varepsilon + 2\varepsilon_m + 2f(\varepsilon - \varepsilon_m)}{\varepsilon + 2\varepsilon_m - f(\varepsilon - \varepsilon_m)} \quad (8)$$

to calculate the effective dielectric constant  $\varepsilon_f$  which gives  $\varepsilon_f \simeq 3$  at  $f = 0.52$  (we take  $\varepsilon_m = 1$ ,  $\varepsilon = 10$  as in the case of CdSe NCs). For these  $\varepsilon_m$  and  $\varepsilon$ , the effective dielectric constant  $\varepsilon_f$  was calculated numerically for all range of  $f$ <sup>23</sup>. One can check that Eq. (8) works well even for  $f$  as large as 0.7. This means that for NCs touching by small facets or separated by short ligands,  $\varepsilon/\varepsilon_f \simeq 3$  is a good estimate for CdSe.

The ratio  $E_c/\Delta$  is an important parameter of our theory. For CdSe with diameter  $d = 5$  nm,  $E_c/\Delta \simeq 1/5$ .

### III. CHARGING OF NANOCRYSTALS DUE TO RANDOM DONOR NUMBERS

Let us now discuss what happens when we bring doped NCs together. At  $n \ll n_c$ , each electron is still localized in a single NC. This localization is related to the major source of disorder in doped NC films, fluctuations of donor numbers  $\delta N$  around the average number  $N$ . At large  $N$ ,  $\delta N$  is Gaussian-distributed, i.e.,  $\delta N = \sqrt{N}$ . If each NC is neutral,  $\delta N$  would lead to substantial fluctuations  $\delta\epsilon_F = \epsilon_F/\sqrt{N} \sim N^{1/6}\Delta$  of the Fermi energy  $\epsilon_F$  from one NC to another. To establish the unique chemical potential of electrons (the Fermi level), electrons move from NCs with larger-than-average  $n$  to ones with smaller-than-average  $n$  and NCs get charged creating the Coulomb potential in space. Below we argue that the typical number of charges  $Q$  in NCs depend on the charging energy  $E_c$  as shown in Fig. 2.

When  $E_c$  is very small, the final unique chemical potential is established when each NC has almost the same number of electrons. Accordingly, most NCs obtain a net charge  $Qe$  where  $Q \sim \sqrt{N}$ . At larger  $E_c$  where

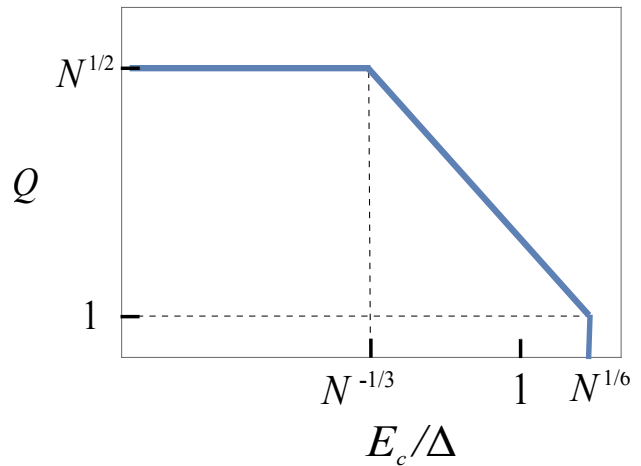


FIG. 2. Schematic log-log plot of the typical number of charges  $Q$  in a NC as a function of the charging energy  $E_c$  measured in units of the energy gap  $\Delta$  between consecutive degenerate  $(n, l)$ -shells.

$E_c/\Delta \gg N^{-1/3}$ , the price of charging gets so large that the number of transferred electrons  $Q \sim N^{1/6}(\Delta/E_c)$  is much smaller than  $\sqrt{N}$  (see Fig. 2). One arrives to this result by equating the initial fluctuation of the Fermi energy  $\delta\epsilon_F$  to the growth of the Coulomb potential  $QE_c$ . At  $E_c/\Delta = N^{1/6}$ , charging becomes so costly that the charge number  $Q = 1$ . Beyond this point, all NCs are neutral (see Fig. 2).

Charging of NCs is the main source of disorder in NC arrays and plays an important role for the electron transport. Each NC finds itself in the environment of charged neighbors and gets a random potential energy shift up or down with respect to its neighbors as  $QE_c$ . It is easy to check by using the charge number  $Q$  calculated above that at  $N^{1/6} > E_c/\Delta > N^{-1/2}$  these random shifts exceed  $\Delta$  so that we arrive at the spacial distribution of levels shown in Fig. 3, which corresponds to a constant density of state. Coulomb correlations "dig" the Coulomb gap in this density of state<sup>15</sup>, which in turn leads to low temperature ES conductivity law Eq. (1). At  $E_c/\Delta > N^{1/6}$  all NCs are neutral (see Fig. 2) so that there is a charging gap  $E_C$  at the Fermi level and the system enters the regime of activated transport<sup>16,21,24</sup>.

At  $E_c/\Delta < N^{-1/2}$ , the energy shifts created by the potential of nearest neighbors are smaller than  $\Delta$ . However, for such small  $E_c$ , the variation of the NC diameter  $\delta d$  can step in and change the energy distance  $\Delta$  between consecutive shells which is  $\propto 1/d^2$  by a ratio  $2(\delta d/d)$ . At not too small  $N$ , e.g., the number of filled shells is larger than 3, the ratio of the final shift of the electron energy levels closest to the Fermi level compared to the energy spacing  $\Delta$  is larger than  $6(\delta d/d) = 30\% - 60\%$  (experimentally,  $\delta d/d$  is as large as  $5 - 10\%$ <sup>25</sup>). So the difference between electron energy levels of neighboring NCs is on the order of  $\Delta$ . As a result, when an electron tunnels between NCs, it is

scattered by intermediate NC states with an energy difference of the order of  $\Delta$  (see Fig. 3).

#### IV. SPLITTING OF DEGENERATE SHELLS

In previous section we dealt with the random potential of randomly charged NCs which shifts the ladder of degenerate levels up and down without splitting them. Here we would like to address the splitting of degenerate levels due to the Stark effect in the random external electric field created by neighboring charged NCs. This field is of the order of  $E \sim e\sqrt{N}/\varepsilon_f d^2$ . Electrons in the NCs respond to the internal field, which is smaller than  $E$  by the factor  $3/(2 + \varepsilon/\varepsilon_f)$ . As we said in Sec. II,  $\varepsilon/\varepsilon_f$  is  $\simeq 3$ , so this factor is  $\simeq 3/5$  and we will ignore it.

To calculate the Stark splitting we first note that the electric field potential matrix element is nonzero only between shells with  $l$  values differing by 1 and is then of the order of  $eEd$ . The typical energy difference between such shells in the spherical well with  $N$  electrons is  $N^{1/3}\Delta$ . Therefore, the typical Stark energy shift or the width of the split shell  $W$  emerges in the second-order perturbation theory and is

$$W \simeq \frac{(eEd)^2}{N^{1/3}\Delta}. \quad (9)$$

(The Stark splitting can also come from random positions of  $N$  donors inside each NC and is comparable to Eq. (9). This disorder creates an internal dipole moment  $\sim \sqrt{N}ed$  and a subsequent electric field, oriented in a random direction.)

Comparing Eq. (9) with the energy gap  $\Delta$  between consecutive shells, we see that at  $E_c/\Delta \simeq N^{-1/3}$  the levels become random with a uniform energy spacing  $\delta = \Delta/N^{1/3}$ . Different  $(n, l)$ -shells mix with each other. Thus inside each NC, the states close to the Fermi level and therefore involved in the electron tunneling have typically different  $l$  numbers<sup>26</sup>. This leads to the case of random spectrum which has been studied in previous work for larger dots<sup>27–31,32</sup>.

In this paper we focus on the case of relatively small  $E_c$ , i.e.,

$$E_c/\Delta < N^{-1/3}, \quad (10)$$

where the degeneracy of levels is still well preserved and the mixing of different  $m$  states due to the electric field can be ignored. Eq. (10) holds for most of realistic situations. For example, in CdSe NCs where one can use  $d = 5$  nm,  $\varepsilon = 10$ ,  $\varepsilon/\varepsilon_f = 3$ ,  $m^* = 0.13m_e$  where  $m_e$  is the free electron mass, one gets  $E_c/\Delta < N^{-1/3}$  at all  $N \ll 100$ . The IMT is expected at  $N \leq 20$  (see Ref. 10) so that we can always think that the inequality (10) is valid. In each  $(n, l)$ -shell, electron states are characterized by the  $m$  number. As we show below, of all these states a single  $m = 0$  level dominates the electron tunneling. It is shown in Fig. 3 by the red color.

So far, we have not talked about the screening of the random electric field by electrons. Since the electron screening radius  $r_0$  can be estimated as  $(\varepsilon_f/4\pi e^2\nu)^{1/2}$  where  $\nu \simeq N^{1/3}/\Delta d^3$  is the average density of states, one gets

$$\frac{r_0}{d} \simeq \left( \frac{N^{-1/3}}{E_c/\Delta} \right)^{1/2}. \quad (11)$$

The ratio  $r_0/d > 1$  when Eq. (10) holds. Thus the electron screening was correctly ignored in our discussion.

#### V. LOCALIZATION LENGTH

At low temperature, the film conductivity is due to the variable-range hopping and obeys ES law Eq. (1). Derivations of ES law assume that each electron is

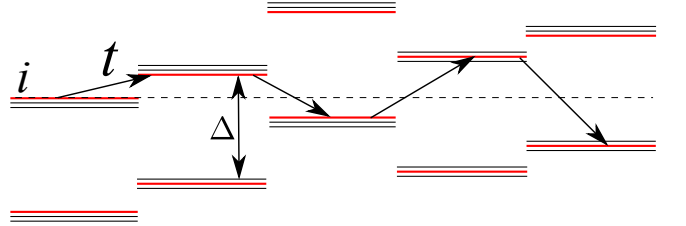


FIG. 3. (Color online) Energy levels close to the Fermi level. An electron tunnels from an initial NC  $i$  through intermediate NCs. The dashed line shows the energy of the tunneling electron. Each NC has a ladder of  $(2l + 1)$ -degenerate  $(n, l)$ -shells with the gap  $\Delta$  between them. Due to charging, the whole ladder of energy levels is shifted up and down by an energy larger than  $\Delta$ . Here we show only two shells closest to the Fermi level. Only one level (red) of the shell contributes to the tunneling with the matrix element  $t$ .

localized in a particular NC and the tunneling matrix element exponentially decays with the distance  $x$  away from its NC as  $\propto e^{-x/\xi}$ . The localization length  $\xi$  is determined by the co-tunneling between two distant NCs with energies close to the Fermi level<sup>28,29,31,33</sup>. In the co-tunneling process, instead of direct hop of one electron from the initial NC to the final one, an electron tunnels between neighboring NCs of the chain of  $M$  intermediate NCs connecting the initial and final NCs. If each incoming electron acquires the same ground energy of the neighboring NC as the outgoing electron had, the co-tunneling process is called elastic. Alternatively, an intermediate NC can acquire an electron-hole excitation. Such process is called inelastic. At low temperatures the elastic process dominates. We show in Sec. VI that in the chain of NCs extended along the  $z$  direction, inside each intermediate NC only the  $m = 0$  state in the highly degenerate  $(n, l)$ -shell contributes to the tunneling process with a dominating matrix element  $t$ . Thus, along a chain of co-tunneling, there is only one possible series of intermediate energy states closest to the energy of the



tunneling electron and no summation over different states is needed in the calculation of the total amplitude. We can say that we deal with non-degenerate levels (red) with the energy spacing  $\Delta$  (see Fig. 3). This allows us to write estimates for the tunneling amplitude as  $\propto (t/\Delta)^M \simeq e^{-x/\xi}$  where  $M = x/d$  is the number of intermediate NCs in the tunneling path and  $\xi$  is the localization length

$$\xi \approx \frac{d}{\ln(\Delta/t)}. \quad (12)$$

Eq. (12) is valid when  $\ln(\Delta/t) \gg 1$  or  $\xi < d$  where the system is far from the critical vicinity of the IMT.

So once the matrix element  $t$  is known, we can get the localization length. Below we calculate the localization length for different types of contacts between NCs which result in different values of  $t$ .

## VI. NANOCRYSTALS TOUCHING BY FACETS

Beyond the surface of a single NC in the surrounding medium, the wavefunction of an electron at the Fermi level decays with the distance  $s$  from the surface as  $\propto e^{-s/b}$  where  $b = \hbar/\sqrt{2mU_0}$ . Here  $m$  is the electron mass in the medium and  $U_0$  is the workfunction of NCs. For  $U_0 \simeq 4$  eV and  $m = m_e$ , where  $m_e$  is the electron mass in vacuum, one gets  $b \simeq 1\text{\AA}$ , which is negligible compared with other lengths. So, approximately, the electron wavefunction is zero on the surface of NCs. When two NCs touch by contact facets, the electron wavefunction of the left NC is strongly modified inside the dashed sphere of radius  $\rho$  containing the facets. Namely, due to the right NC, the wavefunction acquires a tail leaking into the right NC (see Fig. 4a). For the wavefunction inside the right NC, it is deformed in the same way. The overall wavefunction is split into two

$$\Psi_{s,a}(\mathbf{r}) = \frac{1}{\sqrt{2}} [\psi(\mathbf{r} - \mathbf{r}_L) \pm \psi(\mathbf{r} - \mathbf{r}_R)], \quad (13)$$

which are symmetric and asymmetric combinations of the modified wavefunction  $\psi$  inside each NC (see Fig. 4b). The origin is set at the center of the contact and the polar axis is pointed towards the center of the right NC. The coordinates of centers of left and right NCs are  $\mathbf{r}_L$  and  $\mathbf{r}_R$ , respectively.  $\psi(\mathbf{r} - \mathbf{r}_L)$  refers to the wavefunction in the left NC and  $\psi(\mathbf{r} - \mathbf{r}_R)$  is that of the right one. Below, we just use the left wavefunction for discussion and simply denote it as  $\psi$ . The tunneling matrix element  $t$  between two NCs can be estimated by calculating the energy splitting between the symmetric and asymmetric wavefunctions  $\Psi_{s,a}$  of Eq. (13). As in the problem of calculating the electron terms of the molecular ion  $\text{H}_2^+$  in § 81 of Ref. 34, the energy splitting can be calculated as

$$t = \int \frac{\hbar^2}{m^*} \psi \frac{d\psi}{dz} dx dy \quad (14)$$

where the integral is taken over the contact boundary plane  $z = 0$  (see the vertical dashed line in Fig. 4b). In the case we are discussing now, the contact is made of the touching facets. In this contact plane,  $\psi$  vanishes at  $(x, y)$  outside the facets in the surrounding medium.

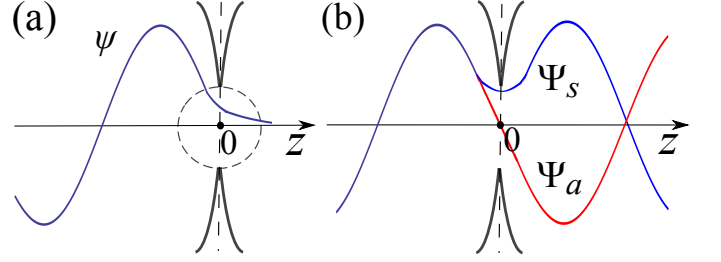


FIG. 4. (Color online) Electron wavefunctions near the contact facet. The vertical dashed line indicates the facet boundary plane. (a) Electron wavefunction  $\psi$  of the left NC modified by the right one. It acquires a tail penetrating into the right NC mainly in the region of the dashed sphere. (b) Overall wavefunction as symmetric (blue) or asymmetric (red) combinations of each NC wavefunction given by Eq. (13). The energy difference between these two states is the tunneling matrix element  $t$  given by Eq. (14).

Let us deal with  $\epsilon_F$  belonging to a degenerate  $(n, l)$ -shell. Then, the unperturbed wave function of the left NC is  $\psi_0(\mathbf{r} - \mathbf{r}_L) \simeq j_l(k_n r') Y_l^m(\theta', \phi') / \sqrt{d/k_n^2}$  where  $j_l$  is the spherical Bessel function,  $Y_l^m$  are spherical harmonics,  $k_n d/2$  is the  $n$ th zero point of the Bessel function and  $k_n \approx 2\pi n/d \sim k_F$ ,  $(r', \theta', \phi')$  are the coordinates of  $\mathbf{r}' = \mathbf{r} - \mathbf{r}_L$  in the spherical coordinate system.  $Y_l^m(\theta', \phi') \rightarrow 0$  at  $\theta' \rightarrow 0$  for all  $m \neq 0$ , and for  $m = 0$   $Y_l^0(0, \phi') = \sqrt{(2l+1)/4\pi} > 0$ . Thus among the  $2l+1$  degenerate levels of the  $(n, l)$ -shell only one state ( $m = 0$ ) oriented along the  $z$  axis contributes to the tunneling between neighboring NCs (marked red in Fig. 3). So we just need to calculate the tunneling matrix element  $t$  of the  $m = 0$  state. When the number  $N$  of electrons inside each NC is large, for the  $(n, l)$ -shell at the Fermi level, we have  $n \sim l \sim N^{1/3} \simeq k_F d$  since the radial and angular kinetic energies should be of the same order. So for the  $m = 0$  state, the wavefunction is highly concentrated near the  $z$  axis spreading mainly within the polar angle  $\simeq 1/\sqrt{k_F d}$ . More accurately, since each  $(n, l)$ -shell has  $2l+1$  degeneracy, we get

$$N \approx 2n(l+1)^2 \sim 2l^3, \quad (15)$$

where the factor 2 comes from the spin degeneracy. As  $N = 4\pi n(d/2)^3/3 = k_F^3 d^3/18\pi$ , we get  $n \sim l \sim (k_F^3 d^3/36\pi)^{1/3}$ . The radial distribution is described by  $j_l(k_n r') \simeq \sin[k_n(r' - d/2)]/k_n r'$  at large  $r'$ . Therefore, we get approximately the normalized unperturbed wavefunction

$$\psi_0 \approx \frac{2 \sin[k_n(r' - d/2)]}{\sqrt{dr'}} Y_l^0(\theta', \phi') \quad (16)$$

at large distance from the left-NC center. So near the facet, the original unperturbed wavefunction  $\psi_0$  can locally be regarded as an incident plane wave superposed by its completely reflected wave from the surface, i.e.,  $\psi_0 \approx 2\sqrt{2l/\pi} \sin[k_n(z' - d/2)]/d^{3/2}$ , where  $z' \approx r'$  is the  $z$ -component of  $\mathbf{r}'$ .

As a result, the problem of an electron tunneling through a facet is analogous to the one of a plane wave with the wavenumber  $k_F$  diffracting on a circular aperture with radius  $\rho$  in  $z = 0$  plane screen. In the regime where  $k_F \rho \ll 1$ , Bethe<sup>35</sup> solved this diffraction problem for microwaves, while Levine and Schwinger<sup>36</sup> and Bouwkamp<sup>37</sup> solved it for a scalar plane wave. Here we use the simple solution in the first-order approximation in  $k_F \rho \ll 1$  given by Rayleigh<sup>38</sup>.

One can write the Schrodinger equation for the function  $\psi$  as

$$\nabla^2 \psi + k_F^2 \psi = 0. \quad (17)$$

Boundary conditions on the  $z = 0$  plane are  $\psi = 0$  on the screen and  $d\psi/dz$  is continuous at the aperture. We write the solution  $\psi$  as the sum of  $\psi_0$  and  $\delta\psi$ , where  $\delta\psi$  is the correction due to the aperture opening and the unperturbed wavefunction  $\psi_0$  of the left NC is zero on the right side of the boundary plane ( $z > 0$ ). We denote  $\delta\psi_L, \delta\psi_R$  as the left ( $z < 0$ ) and right ( $z > 0$ ) part of the correction function  $\delta\psi$  respectively. So in the  $z = 0$  boundary plane,  $\delta\psi_L = \delta\psi_R$  and outside the aperture  $\delta\psi_L = \delta\psi_R = 0$ . The continuity of the derivative  $d\psi/dz$  leads to a jump of  $d(\delta\psi)/dz$ , i.e.,  $d\psi_0/dz + d(\delta\psi_L)/dz = d(\delta\psi_R)/dz$ . The symmetry between  $\delta\psi_L$  and  $\delta\psi_R$  gives  $d(\delta\psi_L)/dz = -d(\delta\psi_R)/dz$  in the aperture (the proof can be found in Refs. 35 and 38. For a possible interpretation of this result, see the footnote<sup>39</sup>) and therefore  $d(\delta\psi_R)/dz = (d\psi_0/dz)/2 \approx \sqrt{2l/\pi} k_n/d^{3/2}$ . Now one can rewrite the integral for  $t$  in terms of the correction to the wave function on the right side which is  $\delta\psi_R$

$$t = \frac{\hbar^2}{m^*} \int \delta\psi_R \frac{d\delta\psi_R}{dz} dx dy, \quad (18)$$

where  $\delta\psi_R$  satisfies the Schrodinger equation (17). At the aperture  $\nabla^2(\delta\psi_R) \sim \delta\psi_R/\rho^2 \gg k_F^2 \delta\psi_R$  because  $k_F \rho \ll 1$ . In the first approximation we can neglect the latter term and thus deal with the Laplace's equation

$$\nabla^2(\delta\psi_R) = 0 \quad (19)$$

with the boundary conditions  $\delta\psi_R = 0$  on the screen and  $d(\delta\psi_R)/dz \approx \sqrt{2l/\pi} k_n/d^{3/2}$  at the aperture.

Mathematically, an identical problem was exactly solved in hydrodynamics (see § 108 in Ref. 40). Indeed, the Laplace's equation  $\nabla^2 \varphi = 0$  can be used to describe the motion of a rigid disk of radius  $\rho$  moving with velocity  $u$  along its axis (defined as the  $z$  axis with the origin at the disk center) through unlimited incompressible liquid

if  $\varphi$  denotes the velocity potential. Boundary conditions for  $\varphi$  are that  $\nabla \varphi = u$  on the disk and  $\varphi = 0$  at  $z = 0$  outside the disk. The kinetic energy of the liquid in the  $z > 0$  space is

$$K = \frac{1}{2} g \int (\nabla \varphi)^2 dV, \quad (20)$$

where  $g$  is the density of the liquid. Using Green's theorem and the Laplace's equation for the right half space ( $z > 0$ ), we get

$$K = \frac{1}{2} g \int \varphi \frac{d\varphi}{dz} dx dy \quad (21)$$

where the integral is taken over the whole  $z = 0$  plane. The potential  $\varphi$  is zero outside the disk. Therefore, the integration is over the disk only, similar to Eq. (18). Knowing the exact solution for  $\varphi$  one can arrive at  $K = (2/3)g\rho^3 u^2$  (see § 108 in Ref. 40). Thus

$$\int \varphi \frac{d\varphi}{dz} dx dy = \frac{4}{3} \rho^3 u^2. \quad (22)$$

In our diffraction problem,  $\delta\psi_R$  plays the role of  $\varphi$  and  $d(\delta\psi_R)/dz \approx \sqrt{2l/\pi} k_n/d^{3/2}$  plays the role of  $u$ . Therefore, using Eq. (6), we get the tunneling matrix element  $t$  in Eq. (18)

$$t = \frac{9\hbar^2 n \rho^3}{m^* d^2} = \frac{0.3\hbar^2 k_F^3 \rho^3}{m^* d^2}. \quad (23)$$

At  $k_F d \sim 1$ , one gets the tunneling matrix element for the 1s band

$$t \simeq \frac{\hbar^2 \rho^3}{m^* d^5}. \quad (24)$$

In Ref. 41, a solution-based oriented attachment method was used to prepare fused dimers of two semiconductor NCs. These dimers can be seen as two NCs touching by their facets. Eq. (24) for  $t$  can then be used to calculate the splitting the first exciton absorption line in the dimer spectrum. One should note that Eq. (24) is obtained here in the limit of infinitesimal tunneling distance  $b$  (which is further explained in Sec. VII). In the same limit, the method used in Ref. 41 leads to a smaller  $t \simeq \hbar^2 \rho^4 / m^* d^6$ . The reason for this difference is that on the facet plane our wavefunction has a larger magnitude than the one conjectured in Ref. 41.

One can interpret the result of tunneling matrix element Eq. (23) as following. Originally the wavefunction  $\psi_0$  is zero on the boundary plane and its derivative along the  $z$  axis is  $\simeq k_F^{3/2}/d$  on the contact facet. Now due to the existence of the facet, the electron wavefunction is modified as  $\psi$  which leaks into the right NC and is nonzero on the facet, while the derivative is hardly changed by the small perturbations. Because the wave function substantially changes over a distance  $\rho$ , we

can say that  $\psi \approx (d\psi/dz)\rho$ . As a result,

$$\begin{aligned} \psi &\simeq \frac{k_F^{3/2} \rho}{d}, \\ \frac{d\psi}{dz} &\simeq \frac{k_F^{3/2}}{d} \end{aligned} \quad (25)$$

inside the contact facet in the  $z = 0$  plane for the  $m = 0$  state which is highly oriented along the  $z$  axis. So we get the result (23) for  $t$ .

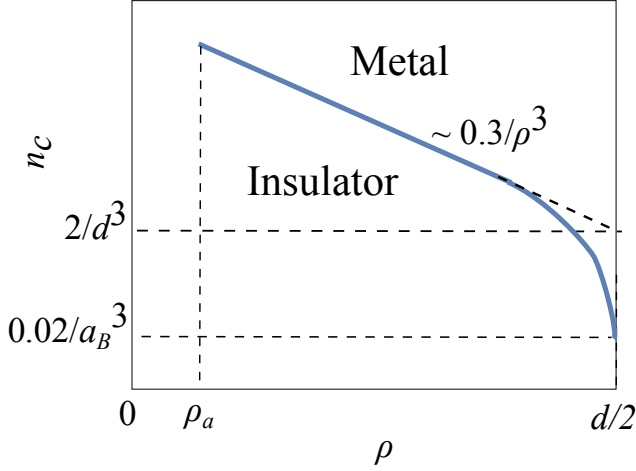


FIG. 5. Schematic logarithmic plot of the critical concentration  $n_c$  as a function of the facet radius  $\rho$  at  $a_B \gg d$ . Both axes use logarithmic scales. Near  $\rho = d/2$ , the critical concentration abruptly drops to its value for bulk semiconductors.

Now we can calculate the localization length by using Eqs. (5) and (12) and arrive at the estimate Eq. (4). Our result for  $\xi$  is obtained away from the critical vicinity of  $n_c$ . Indeed we were estimating the probability of the electron hopping between two distant NCs mediated by the elastic co-tunneling along a single typical chain of  $M$  NCs. Near the IMT one should add probability amplitudes of many such chains. Then the sum of all amplitudes gives a total probability  $\propto (tK/\Delta)^M$ . Here  $K$  is the connective constant of the NC lattice. According to Anderson<sup>42</sup>, the IMT happens when  $tK/\Delta = 1$ . Using Eqs. (5) and (23), for the simple cubic lattice (where according to Ref. 43  $K = 4.7$ ) we arrive at the estimate  $n_c \approx 0.5\rho^{-3}$  while for the face-centered cubic lattice (where  $K = 10$  as given in Ref. 44) we get  $n_c \approx 0.2\rho^{-3}$ . These results from the insulating side of the IMT are reasonably close to Eq. (3) obtained from the metallic side.

A schematic plot of  $n_c$  as a function of  $\rho$  is presented in Fig. 5. The critical concentration scales as  $\simeq 0.3/\rho^3$  at all  $\rho \ll d/2$ . In the vicinity of  $\rho = d/2$ , electrons are no longer confined inside each NC and the film becomes a bulk semiconductor. In this case,  $n_c a_B^3 \simeq 0.02$ , we return to the Mott criterion for the IMT and get a drastic drop of the critical concentration from  $\simeq 2/d^3$  to  $0.02/a_B^3$ .

## VII. NANOCRYSTALS TOUCHING AWAY FROM FACETS

When NCs touch each other away from prominent facets but by an area of the atomic size  $a \ll \rho$ , the electrons tunnel mainly via the effective “ $b$ -contact” of radius  $\rho_b = \sqrt{db/2} \gg a$  (see Fig. 6). For electrons tunneling between NCs outside this contact, the tunneling distance is larger than  $b$  and the probability is negligible due to the exponentially decaying wavefunction. Since electrons have to tunnel through the

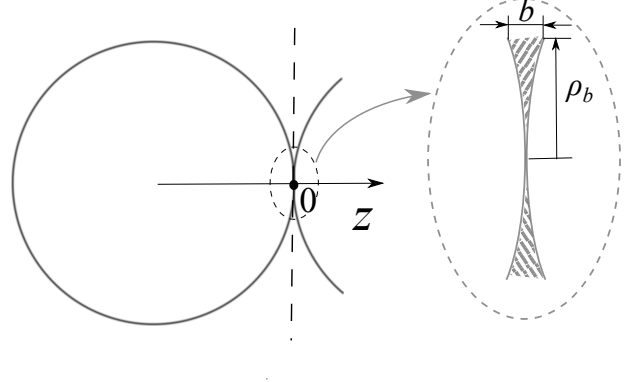


FIG. 6. Two NCs touching away from prominent facets. In this case, electrons tunnel through the  $b$ -contact shown in the inset.

medium of which the electron mass is  $m$ , when repeating the integral Eq. (14) over the contact boundary plane here, we need to replace the effective mass  $m^*$  with  $m$

$$t = \int \frac{\hbar^2}{m} \psi \frac{d\psi}{dz} dx dy. \quad (26)$$

In this case we can use the LCAO approximation in the way done for the ground state in Ref. 19. We calculate  $\psi = \psi_0$  as the wavefunction for a single spherical NC embedded in the infinite surrounding medium with the finite decay length  $b$ . For simplicity, in this section and below we do only scaling analysis ignoring numerical coefficients.

Using the continuity of the wavefunction on the NC surface, we get

$$\psi_0 \simeq \frac{k_F}{\sqrt{d}} Y_l^m(\theta', \phi') \begin{cases} j_l(k_F r') & r' < \frac{d}{2} \\ \frac{j_l(k_F d/2)}{h_l^{(1)}(id/2b)} h_l^{(1)}(ir'/b) & r' > \frac{d}{2}, \end{cases} \quad (27)$$

where  $h_l^{(1)}$  is the first-kind spherical Hankel function and only  $Y_l^0(\theta', \phi')$  is nonzero at  $\theta' = 0$  corresponding to the state participating in the tunneling. The origin is set at the touching point of NCs with the  $z$  axis pointed towards the center of the right NC and therefore the boundary plane is at  $z = 0$  (see the vertical dashed line in Fig. 6). Again  $(r', \theta', \phi')$  are the coordinates of

$\mathbf{r}' = \mathbf{r} - \mathbf{r}_L$  in the spherical coordinate system and  $\mathbf{r}_L$  is the coordinate of the center of the left NC. Since for a finite potential barrier which is the work function  $U_0$  here the derivative of the wavefunction divided by the effective mass is continuous across the surface, we have

$$\left. \frac{d\psi_0}{dr'} \frac{1}{m^*} \right|_{r'-d/2=0^-} = \left. \frac{d\psi_0}{dr'} \frac{1}{m} \right|_{r'-d/2=0^+}. \quad (28)$$

Using that  $j_l(k_F r') \simeq \sin[k_F r' + \varphi_l]/k_F r'$ ,  $h_l^{(1)}(i r'/b) \simeq b e^{-r'/b}/r'$  at large  $r'$  near the surface where  $\varphi_l$  is a constant, we have

$$\cot\left(\frac{k_F d}{2} + \varphi_l\right) \simeq -\frac{m^*}{m k_F b} + \frac{2}{k_F d} \quad (29)$$

where  $d/b \gg 1$ ,  $m/m^* \gg 1$ ,  $k_F d \gg 1$  at high doping concentration and  $k_F d \sim 1$  for the ground state. At  $1/k_F b \gg m/m^*$ , the cotangent function diverges which means  $\cos(k_F d/2 + \varphi_l) \approx 1$ ,  $1/\sin(k_F d/2 + \varphi_l) \approx -m^*/m k_F b$ . So on the boundary plane inside the  $b$ -contact ( $r' - d/2 = 0^+$ ), we have

$$\begin{aligned} \psi_0 &\simeq \frac{-k_F}{\sqrt{d}} \frac{m k_F b}{k_F d m^*} \sqrt{l} \\ \frac{d\psi_0}{dr} &\simeq \frac{k_F}{\sqrt{d}} \frac{m k_F}{k_F d m^*} \sqrt{l}. \end{aligned} \quad (30)$$

The tunneling matrix element is then

$$t \simeq \frac{\hbar^2 k_F^3 d b^2 (m/m^*)}{m^* d^2}. \quad (31)$$

At  $1/k_F b \ll m/m^*$ , the cotangent function either vanishes or is finite depending on whether  $d/b \gg m/m^*$  or  $k_F d \gg 1$  is satisfied. This means the sine function is always finite and of the order 1. So inside the  $b$ -contact we get

$$\begin{aligned} \psi_0 &\simeq \frac{k_F}{\sqrt{d}} \frac{1}{k_F d} \sqrt{l} \\ \frac{d\psi_0}{dr} &\simeq \frac{-k_F}{\sqrt{d}} \frac{1}{k_F d b} \sqrt{l}, \end{aligned} \quad (32)$$

and the tunneling matrix element is

$$t \simeq \frac{\hbar^2 k_F d (m^*/m)}{m^* d^2}. \quad (33)$$

One can check that when we put  $k_F^{-1} \sim d$  into Eqs. (31) and (33), we get the same tunneling matrix elements for the ground state as derived in Ref. 19 for touching NCs.

According to Eqs. (31) and (33), the localization length is then

$$\xi \approx \begin{cases} \frac{d}{\ln[1/n d b^2 (m/m^*)]}, & \frac{m}{m^*} \ll \frac{1}{n^{1/3} b} \\ \frac{d}{\ln[1/n^{1/3} d (m^*/m)]}, & \frac{m}{m^*} \gg \frac{1}{n^{1/3} b}. \end{cases} \quad (34)$$

This leads to the critical concentration

$$n_c \simeq \begin{cases} \frac{1}{b^2 d} \frac{m^*}{m}, & \frac{m}{m^*} \ll \left(\frac{d}{b}\right)^{1/2} \\ \frac{1}{d^3} \left(\frac{m}{m^*}\right)^3, & \frac{m}{m^*} \gg \left(\frac{d}{b}\right)^{1/2} \end{cases} \quad (35)$$

which has its minimum value  $n_c \simeq 1/(db)^{3/2} = 1/\rho_b^3$  at  $m/m^* \simeq \sqrt{d/b}$ . Even this minimum value is much larger than  $1/\rho_a^3$  since  $\rho_a \gg \rho_b$ . Thus, when NCs touch away from prominent facets the critical concentration is pushed much higher. In fact, for CdSe NC films, by using  $b = 0.1$  nm,  $d = 5$  nm,  $m = m_e$ ,  $m^* = 0.13 m_e$ ,<sup>45</sup> where  $m_e$  is the free electron mass, we get  $n_c \simeq 3 \times 10^{21} \text{cm}^{-3}$  which is probably difficult to achieve.

One can think that when we put  $\rho = \rho_b \approx \sqrt{db/2}$  into Eq. (4) which is calculated for NCs touching by facets of radius  $\rho$ , we should get the localization length for NCs touching by the effective “ $b$ -contact”. However, the actual  $\xi$  according to Eq. (34) is different from this value. For a relatively small mass ratio  $m/m^* \ll 1/n^{1/3} b$ , this is because the characteristic length which determines the amplitude of the wavefunction on the contact is  $bm/m^*$  instead of  $\rho_b$ . Again, locally the electron wavefunction can be regarded as an incident plane wave superposed by its reflected wave from the surface. The ratio of the nonzero wavefunction on the contact compared to the amplitude of the incident wave is  $k_F$  multiplied by this characteristic length. In Sec. VI, the only characteristic length related to the contact is its radius  $\rho$  while here it is the decay length  $b$  of the wavefunction outside the NC multiplied by the mass ratio  $m/m^*$  promoting the electron tunneling. At  $m/m^* \gg 1/n^{1/3} b$ , the enhancing effect of the mass ratio saturates. The localization length is different from the one got from Eq. (4) with  $\rho = \rho_b$  because the wavefunction on the contact does not depend on the radius  $\rho_b$  as can be seen from Eq. (32). One should note however that the localization length given by Eq. (34) can be larger than that of Eq. (4). When  $m/m^* \simeq 1/n^{1/3} b \simeq 1/k_F b$ , the localization length of electrons tunneling via the  $b$ -contact reaches its maximum value as

$$\xi \approx \frac{d}{\ln(1/k_F^2 b d)}. \quad (36)$$

This localization length is much larger than that of electrons tunneling via contact facets as given by Eq. (4) when

$$\rho^3 \ll \frac{b d}{k_F}. \quad (37)$$

This is because at small  $k_F$ , due to the large size of the electron wave packet  $\sim k_F^{-1}$ , the diffraction probability of electrons through the contact is very small. However, when electrons tunnel via the  $b$ -contact, the probability is increased considerably by the big mass



ratio  $m/m^*$ . This results in a larger tunneling matrix element between NCs despite the smaller radius  $\rho_b$  of the contact. Experimentally, nevertheless, this condition Eq. (37) is very hard to realize. For example, in CdSe NC films where one can use  $b = 0.1$  nm,  $d = 5$  nm,  $m^*/m = 0.13$ ,  $\rho = \rho_a = \sqrt{da/2} = 1.2$  nm, at  $1/k_F b \simeq m/m^*$ , Eq. (37) is strongly violated. Therefore, in reality the electron tunneling via the  $b$ -contact is much weaker than that through the facet. This means the failure of the LCAO approach in the case where NCs touch by facets, and justifies our results of the tunneling matrix element and the localization length in that situation.

When NCs are separated by short ligands to a distance  $s^{46}$ , the overlapping wavefunctions exponentially decay as  $\propto e^{-s/b}$  between neighboring NCs. So the localization length satisfies that  $e^{-d/\xi} \simeq e^{-s/b}$  which means  $\xi \simeq bd/s$ . More careful calculations can give the prefactor of this exponential decaying component  $e^{-s/b}$  of the wavefunction. Following a procedure similar to above derivations, we can get the tunneling matrix element  $t$  as

$$t \simeq \frac{\hbar^2}{m^* d^2} \exp\left(-\frac{s}{b}\right) \begin{cases} k_F^3 b^2 d \frac{m}{m^*}, & \frac{m}{m^*} \ll \frac{1}{k_F b} \\ k_F d \frac{m^*}{m}, & \frac{m}{m^*} \gg \frac{1}{k_F b} \end{cases} \quad (38)$$

which again, by replacing  $k_F$  with  $1/d$ , gives the same results as in Ref. 19 but for NCs separated by short ligands.

Therefore, we get the localization length with the logarithmic correction

$$\xi \approx \begin{cases} \frac{d}{s/b + \ln[1/ndb^2(m/m^*)]}, & \frac{m}{m^*} \ll \frac{1}{n^{1/3}b} \\ \frac{d}{s/b + \ln[1/n^{1/3}d(m^*/m)]}, & \frac{m}{m^*} \gg \frac{1}{n^{1/3}b}. \end{cases} \quad (39)$$

For small  $s$ , near the IMT, the role of the correction becomes important. One should note that even

when NCs touch by short ligands, the localization length of electrons can be enhanced by increasing the doping concentration  $n$  inside each NC. The critical concentration  $n_c$  is then

$$n_c \simeq \begin{cases} \frac{1}{b^2 d} \frac{m^*}{m} \exp\left(\frac{s}{b}\right), & s \ll b \ln \left[ \left(\frac{m^*}{m}\right)^2 \frac{d}{b} \right] \\ \frac{1}{d^3} \left(\frac{m}{m^*}\right)^3 \exp\left(\frac{3s}{b}\right), & s \gg b \ln \left[ \left(\frac{m^*}{m}\right)^2 \frac{d}{b} \right] \end{cases} \quad (40)$$

which can easily become unrealistically large.

## VIII. CONCLUSION

In this paper we have studied the electron localization length  $\xi$  of NC films when the electron spectrum in NCs has highly degenerate energy shells. We find  $\xi(n)$  as a function of the electron doping concentration  $n$  inside each NC. We have investigated the case when NCs touch each other by contact facets and got the  $\xi(n)$  dependence which qualitatively confirms the IMT criterion obtained in previous work<sup>10</sup>. We have also studied the cases when NCs touch away from prominent facets or are separated by short ligands. To make our analyses more complete, we studied the non-degenerate case where the energy shells are strongly split by the disorder potential caused by random donor positions. We talked about the localization length at low doping concentration as well and found the crossover to the behavior at high concentration.

### Acknowledgments.

We are grateful to I. S. Beloborodov, A. S. Ioselevich, A. Kamenev, U. R. Kortshagen, B. Skinner, Al. L. Efros, and K. A. Matveev for helpful discussions. This work was supported primarily by the National Science Foundation through the University of Minnesota MRSEC under Award No. DMR-1420013.

\* fuxxx254@umn.edu

<sup>1</sup> I. Gur, N. A. Fromer, M. L. Geier, and A. P. Alivisatos, *Science* **310**, 462 (2005).

<sup>2</sup> V. Wood and V. Bulovic, *Nano Reviews* **1**, 5202 (2010).

<sup>3</sup> M. E. Turk *et al.*, *Nano Lett.* **14**, 5948 (2014).

<sup>4</sup> R. Gresback, N. J. Kramer, Y. Ding, T. Chen, U. R. Kortshagen, and T. Nozaki, *ACS Nano* **8**, 5650 (2014).

<sup>5</sup> A. P. Alivisatos, *Science* **271**, 933 (1996).

<sup>6</sup> E. H. Sargent, *Nature Photonics* **3**, 325 (2009).

<sup>7</sup> C. B. Murray, D. J. Norris, and M. G. Bawendi, *Journal of the American Chemical Society* **115**, 8706 (1993).

<sup>8</sup> C. Wang, M. Shim, and P. Guyot-Sionnest, *Science* **291**, 2390 (2001).

<sup>9</sup> D. Yu, C. Wang, and P. Guyot-Sionnest, *Science* **300**, 1277 (2003).

<sup>10</sup> T. Chen, K. V. Reich, N. J. Kramer, H. Fu, U. R. Kortshagen, and B. I. Shklovskii, *Nat. Mater.* (2015), 10.1038/nmat4486.

<sup>11</sup> H. Liu, A. Pourret, and P. Guyot-Sionnest, *ACS Nano* **4**, 5211 (2010).

<sup>12</sup> A. J. Houtepen, D. Kockmann, and D. Vanmaekelbergh, *Nano Lett.* **8**, 3516 (2008).

<sup>13</sup> D. Mocatta, G. Cohen, J. Schattner, O. Millo, E. Rabani, and U. Banin, *Science* **332**, 77 (2011).

<sup>14</sup> A. Sahu *et al.*, *Nano Letters* **12**, 2587 (2012).

<sup>15</sup> A. L. Efros and B. I. Shklovskii, *J. Phys. C: Solid State*

- Phys. **8**, L49 (1975).
- <sup>16</sup> B. Skinner, T. Chen, and B. I. Shklovskii, Phys. Rev. B **85**, 205316 (2012).
  - <sup>17</sup> D. J. Norris, A. L. Efros, and S. C. Erwin, Science **319**, 1776 (2008).
  - <sup>18</sup> P. Guyot-Sionnest, J. Phys. Chem. Lett. **3**, 1169 (2012).
  - <sup>19</sup> A. Shabaev, A. L. Efros, and A. L. Efros, Nano Lett. **13**, 5454 (2013).
  - <sup>20</sup> M. Scheele, Zeitschrift für Physikalische Chemie **229**, 167 (2015).
  - <sup>21</sup> T. Chen, B. Skinner, W. Xie, B. I. Shklovskii, and U. R. Kortshagen, J. Phys. Chem. C **118**, 19580 (2014).
  - <sup>22</sup> J. Maxwell, *A treatise on electricity and magnetism*, Vol. 2 (Clarendon, Oxford, 1891).
  - <sup>23</sup> L. C. Shen, C. Liu, J. Kortinga, and K. J. Dunn, Journal of Applied Physics **67**, 7071 (1990).
  - <sup>24</sup> In Ref. 16, the border between the ES and activated transport regimes was found to be  $E_c/\Delta \sim 1$  at  $N < 8$ . Here we generalized this result to the large  $N$  case and obtained  $E_c/\Delta \sim N^{1/6}$  for this border.
  - <sup>25</sup> C. B. Murray, C. R. Kagan, and M. G. Bawendi, Annual Review of Materials Science **30**, 545 (2000).
  - <sup>26</sup> Recall that different  $l$  states have different parity, this means that the corresponding tunneling matrix element  $t$  has random signs.
  - <sup>27</sup> I. S. Beloborodov, K. B. Efetov, A. V. Lopatin, and V. M. Vinokur, Phys. Rev. Lett. **91**, 246801 (2003).
  - <sup>28</sup> M. V. Feigel'man and A. S. Ioselevich, JETP Lett. **81**, 277 (2005).
  - <sup>29</sup> I. S. Beloborodov, A. V. Lopatin, and V. M. Vinokur, Phys. Rev. B **72**, 125121 (2005).
  - <sup>30</sup> L. I. Glazman and M. Pustilnik, *Nanophysics: Coherence and Transport*, 427 (2005).
  - <sup>31</sup> I. S. Beloborodov, A. V. Lopatin, V. M. Vinokur, and K. B. Efetov, Rev. Mod. Phys. **79**, 469 (2007).
  - <sup>32</sup> One may note that this criterion for degeneracy lifting is different from the one in Ref. 10. However, since the critical concentration  $n_c$  has the same expression in both degenerate and nondegenerate cases, this does not affect the correctness of the metal-insulator transition criterion obtained in Ref. 10.
  - <sup>33</sup> J. Zhang and B. I. Shklovskii, Phys. Rev. B **70**, 115317 (2004).
  - <sup>34</sup> L. D. Landau and E. M. Lifshitz, *Quantum Mechanics (Non-relativistic Theory)*, edited by E. M. Lifshitz and L. P. Pitaevskii, Course of Theoretical Physics, Vol. 3 (Butterworth-Heinemann, 1991).
  - <sup>35</sup> H. A. Bethe, Phys. Rev. **66**, 163 (1944).
  - <sup>36</sup> H. Levine and J. Schwinger, Phys. Rev. **74**, 958 (1948).
  - <sup>37</sup> C. J. Bouwkamp, Reports on Progress in Physics **17**, 35 (1954).
  - <sup>38</sup> F. R. S. Rayleigh, Philosophical Magazine Series 5 **43**, 259 (1897).
  - <sup>39</sup> Let us consider the standing-wave solution of Shrodinger equation Eq. (17) in a free space:  $\psi = \exp(ik_F z) - \exp(-ik_F z)$ . Since  $\psi = 0$  at  $z = 0$ , this means that  $\psi$  is also the solution of the Shrodinger equation if the screen is located at  $z = 0$ . This solution can be viewed as two plane waves  $\exp(ik_F z)$  and  $-\exp(-ik_F z)$ , which fall from opposite directions on the screen and are reflected back completely. The aperture gives rise to corrections  $\delta\psi_R$  and  $\delta\psi_L$  to each wave. Since the screen does not affect the wavefunction  $\psi$ , these corrections to plane waves cancel each other, i.e.  $\delta\psi_R(z) - \delta\psi_L(-z) = 0$ . By differentiating this relation we get that  $d(\delta\psi_R)/dz = -d(\delta\psi_L)/dz$ .
  - <sup>40</sup> H. Lamb, *Hydrodynamics* (Cambridge: University Press, 1895).
  - <sup>41</sup> B. K. Hughes, J. L. Blackburn, D. Kroupa, A. Shabaev, S. C. Erwin, A. L. Efros, A. J. Nozik, J. M. Luther, and M. C. Beard, Journal of the American Chemical Society **136**, 4670 (2014).
  - <sup>42</sup> P. W. Anderson, Proceedings of the National Academy of Sciences **69**, 1097 (1972).
  - <sup>43</sup> N. Clisby, Journal of Physics A: Mathematical and Theoretical **46**, 245001 (2013).
  - <sup>44</sup> S. McKenzie, Journal of Physics A: Mathematical and General **12**, L267 (1979).
  - <sup>45</sup> J. O. Dimmock and R. G. Wheeler, Journal of Applied Physics **32**, 2271 (1961).
  - <sup>46</sup> D. V. Talapin and C. B. Murray, Science **310**, 86 (2005).